ResearchGate

See discussions, stats, and author profiles for this publication at: https://www.researchgate.net/publication/6015229

First principles molecular dynamics of molten NaI: Structure, self-diffusion, polarization effects, and charge transfer

ARTICLE *in* THE JOURNAL OF CHEMICAL PHYSICS · OCTOBER 2007

Impact Factor: 2.95 · DOI: 10.1063/1.2768968 · Source: PubMed

CITATIONS
11

READS
63

2 AUTHORS:

Nuno Galamba

24 PUBLICATIONS **311** CITATIONS

SEE PROFILE

Benedito J. Costa Cabral

43 PUBLICATIONS **794** CITATIONS

SEE PROFILE

Available from: Nuno Galamba
Retrieved on: 26 January 2016

First principles molecular dynamics of molten NaI: Structure, self-diffusion, polarization effects, and charge transfer

N. Galamba and B. J. Costa Cabral

Citation: The Journal of Chemical Physics **127**, 094506 (2007); doi: 10.1063/1.2768968
View online: http://dx.doi.org/10.1063/1.2768968
View Table of Contents: http://scitation.aip.org/content/aip/journal/jcp/127/9?ver=pdfcov
Published by the AIP Publishing

This article is copyrighted as indicated in the article. Reuse of AIP content is subject to the terms at: http://scitation.aip.org/termsconditions. Downloaded to IP: 194.117.6.7 On: Sat, 21 Dec 2013 23:21:23

First principles molecular dynamics of molten NaI: Structure, self-diffusion, polarization effects, and charge transfer

N. Galamba[a)]
Grupo de Física-Matemática da Universidade de Lisboa, Avenue Professor Gama Pinto 2, 1649-003 Lisboa, Portugal

B. J. Costa Cabral
Departmento de Química e Bioquímica, Faculdade de Ciências da Universidade de Lisboa, 1749-016 Lisboa, Portugal and Grupo de Física-Matemática da Universidade de Lisboa, Avenue Professor Gama Pinto 2, 1649-003 Lisboa, Portugal

(Received 18 June 2007; accepted 13 July 2007; published online 5 September 2007)

The structure and self-diffusion of NaI and NaCl at temperatures close to their melting points are studied by first principles Hellmann-Feynman molecular dynamics (HFMD). The results are compared with classical MD using rigid-ion (RI) and shell-model (ShM) interionic potentials. HFMD for NaCl was reported before at a higher temperature [N. Galamba and B. J. Costa Cabral, J. Chem. Phys. **126**, 124502 (2007)]. The main differences between the structures predicted by HFMD and RI MD for NaI concern the cation-cation and the anion-cation pair correlation functions. A ShM which allows only for the polarization of I^- reproduces the main features of the HFMD structure of NaI. The inclusion of polarization effects for both ionic species leads to a more structured ionic liquid, although a good agreement with HFMD is also observed. HFMD Green-Kubo self-diffusion coefficients are larger than those obtained from RI and ShM simulations. A qualitative study of charge transfer in molten NaI and NaCl was also carried out with the Hirshfeld charge partitioning method. Charge transfer in molten NaI is comparable to that in NaCl, and results for NaCl at two temperatures support the view that the magnitude of charge transfer is weakly state dependent for ionic systems. Finally, Hirshfeld charge distributions indicate that differences between RI and HFMD results are mainly related to polarization effects, while the influence of charge transfer fluctuations is minimal for these systems. © *2007 American Institute of Physics*. [DOI: 10.1063/1.2768968]

I. INTRODUCTION

Polarization effects and charge transfer are of great interest in understanding the structure and dynamics of ionic systems. The way these two effects can be coupled and correctly accounted for in interionic potentials is still an unresolved issue. Polarization effects (induction forces) cannot be accounted for through pairwise additive potentials. Moreover, the polarizability of ionic species in condensed phase, needed to describe polarization effects and also van der Waals interactions, is a difficult property to extract both from experiment and theory. Therefore, some specific questions concerning the structure and dynamics of molten salts deserve further investigation. A fundamental problem concerns the influence of polarization effects on the like ion partial radial distribution functions of molten alkali halides. Neutron diffraction and isotopic substitution techniques allowed Edwards *et al.*[1] to extract from the total structure factor of molten NaCl ($T=1148$ K) the partial radial distribution functions. Their results show a small but significant difference between $g_{++}(r)$ and $g_{--}(r)$, specifically, the height of the peaks for the like ion correlations, obey the relation $g_{--}(r)>g_{++}(r)$ and for the position of the first maximum $r_{--}>r_{++}$. These results are in contradiction with simulation studies[2] based on the Born-Mayer-Huggins-Tosi-Fumi[3–7] (BMHTF) rigid-ion (RI) interionic potential for molten NaCl, which predicts almost no differences between the like ion partial functions. Molecular dynamics (MD) simulations of the shell model (ShM) for molten NaCl,[8,9] in turn, predict an exaggerated separation between $g_{++}(r)$ and $g_{--}(r)$ relative to the neutron diffraction results. Biggin and Enderby[10] recalculated the partial radial distribution functions from the same total structure factor obtained by Edwards *et al.*[1] but using a different scattering amplitude for the isotope of chlorine ^{37}Cl. While general conclusions about the structure of molten NaCl remain unchanged in that work, the authors state that, to within the accuracy of the measurements, $g_{++}(r)$ and $g_{--}(r)$ are identical.

The differences between $g_{++}(r)$ and $g_{--}(r)$ predicted by the BMHTF RI effective potential for molten alkali halides are controlled by the repulsive Coulombic interactions and the ionic radii of the positive and negative species through the overlap repulsion term.[11] Thus, like ion pair correlation functions for molten salts such as KCl (Ref. 12) and NaCl (Ref. 2) are almost identical. The differences in $g_{++}(r)$ and $g_{--}(r)$ predicted by shell model[8,9,13,14] and other polarizable

a)Author to whom all correspondence should be addressed. Electronic mail: ngalamba@cii.fc.ul.pt

 © 2007 American Institute of Physics

This article is copyrighted as indicated in the article. Reuse of AIP content is subject to the terms at: http://scitation.aip.org/termsconditions. Downloaded to IP: 194.117.6.7 On: Sat, 21 Dec 2013 23:21:23

models[14,15] that take account of Coulombic and overlap repulsion induction forces are therefore attributed to polarization effects.

Regarding the problem of charge transfer effects on the structure and dynamics of ionic liquids, this is normally absent from both RI and polarizable interionic potentials. The magnitude of charge transfer is not an experimental nor a quantum mechanics observable. The electronic (charge) density is the directly related observable that can be obtained from electronic structure calculations. Thus any definition of ionic charge used in any potential model is always to some point arbitrary. This, in addition to the fact that the charge transfer is a many-body effect, makes the introduction of charge transfer mechanisms in classical simulations an especially difficult problem. For the specific case of alkali halides, charge transfer is almost always assumed to be complete, that is, the values +1 and −1 are used for the alkali metals and halides, respectively.

Even though charge transfer is likely to be close to complete for alkali halides, charge fluctuations must take place since electronic density changes with the nuclear motion. A number of questions arise from this observation. What is the size of the fluctuations of atomic charges for a given system? What is the charge transfer magnitude dependence on the thermodynamic state? What is the effect of charge fluctuations on the structure and dynamics of an ionic liquid? These points become especially relevant for systems in which large deviations from a full ionic description are expected. For such systems, interionic potentials may even become state dependent.

The most adequate method for a correct description of both polarization effects and charge transfer is first principles molecular dynamics. First principles Hellmann-Feynman MD (HFMD) calculations for molten NaCl at a single state point ($T=1528$ K) were recently reported by Galamba and Costa Cabral,[16] and a close agreement with experimental data was observed for the structure and self-diffusion coefficients of the ionic species. Regarding the separation of $g_{++}(r)$ and $g_{--}(r)$, HFMD results are in good agreement with the experimental results of Edwards *et al.*,[1] thus keeping with the idea that polarization effects explain this separation. Again, this conclusion is tied to the assumption that charge transfer is close to complete and ionic charge fluctuations do not affect the structure of molten alkali halides.

In the present work, we extend our HFMD calculations to a system (NaI) with a high polarizability anion, the iodide anion, and report on a new state point for NaCl at a much lower temperature. We compare the HFMD results with MD simulations of the BMHTF RI effective potential and with the adiabatic shell model[17] using parameters of Sangster and Dixon.[9] We investigate the performance of two shell models: in the first one only I^- is polarizable[9,13] and in the second both ionic species (Na^+ and I^-) are polarizable.[9] We also report an analysis of the ionic charge distribution and transfer in NaI and NaCl based on the Hirshfeld charge partitioning scheme.[18]

The article is organized as follows. In Sec. II we give a description of the technical details on the HFMD and the RI and ShM MD simulations. The results for the structure, self-diffusion coefficients, and Hirshfeld charge calculations for NaI and NaCl are discussed in Sec. III. The conclusions of this study are given in Sec. IV.

II. MOLECULAR DYNAMICS SIMULATIONS

In this section we explain some of the technical details involved on both HFMD and classical MD of RI and the adiabatic ShM carried for molten NaI and NaCl.

A. Hellmann-Feynman MD

The method used in this work to perform HFMD was described before for the case of molten NaCl.[16] Hellmann-Feynman MD is based on density functional theory[19,20] (DFT) calculations with pseudopotentials and plane waves. The Kohn-Sham equations in the plane-wave representation and periodic boundary conditions are solved self-consistently for the ground state of the pseudoatoms every time step. The Hellmann-Feynman forces are calculated using the program ABINIT, and a molecular dynamics code developed by the authors is coupled to ABINIT to generate a trajectory in the phase space under microcanonical (N,V,E) conditions. The ABINIT code is a common project of the Université Catholique de Louvain, Corning Incorporated, and other contributors. ABINIT relies on an efficient fast Fourier transform algorithm[21] for the conversion of wave functions between real and reciprocal spaces, on the adaptation to a fixed potential of the band-by-band conjugate-gradient method,[22] and on a potential-based conjugate-gradient algorithm for the determination of the self-consistent potential.[23]

The HFMD of NaI and NaCl were carried out at the Γ point, and the kinetic energy cutoff of the plane wave basis set expansion was chosen to be 35 hartrees after preliminary convergence studies. The Perdew-Burke-Ernzerhof[24] (PBE) generalized gradient approximation (GGA) functional was used for the exchange-correlation (XC) energy. The tolerance of the self-consistent field convergence was defined on the forces with a value of 10^{-4} hartree/bohr. Norm-conserving PBE-GGA pseudopotentials of the Troullier-Martins[25] (TM) type were chosen, with nonlinear-core-valence XC (Ref. 26) correction for the atom of sodium. The pseudopotentials are those available at ABINIT obtained with the FHI98PP code.[27] A system composed of 64 atoms (32 atoms of I or Cl and 32 atoms of Na) was considered for both NaI and NaCl, and the starting configurations were equilibrated (1500 time steps with a time step of 5 fs) configurations of the BMHTF RI potential for molten NaI and NaCl. Newton's equations of motion were solved by a Verlet "leapfrog" algorithm with a time step of 5 fs. The chosen temperatures and the corresponding experimental densities[28] were, for NaI, $T=1050$ K and $\rho=2.6308$ g cm^{-3} and, for NaCl, $T=1100$ K and $\rho=1.5420$ g cm^{-3}. Further equilibration of the system was carried out by HFMD for 500 time steps (2.5 ps). The velocities were scaled for the desired temperatures every 5 time steps during the first 300 time steps. The production part of the simulation was carried out for 8.5 ps (1700 time steps). The total energy was conserved within the limits of accuracy of the calculations. The final average temperatures of the HFMD simulations were, respectively, $T=995$ and 1058 K

This article is copyrighted as indicated in the article. Reuse of AIP content is subject to the terms at: http://scitation.aip.org/termsconditions. Downloaded to IP: 194.117.6.7 On: Sat, 21 Dec 2013 23:21:23

for NaI and NaCl. The melting point of NaI is 935 K and that of NaCl is 1074 K, and therefore the average temperature for NaCl is slightly below its melting temperature.

B. Rigid-ion and shell-model MD

The RI and ShM MD simulations were performed for 216 ions (108 I^- or Cl^- and 108 Na^+). The ShM parameters for both NaI and NaCl are those of Sangster and Dixon[9] given in their Table 8, which allow for polarization of both ionic species. Sangster and Dixon[9] criticized their own shell-model parametrization for the case of sodium halides. This criticism was based on the results obtained for the charge of the Na^+ shells, which differs markedly from those for the K^+ and Rb^+ halides when polarization effects are taken into account for both ions. The authors considered that perhaps it would be adequate to consider only one ion to be polarizable, at least for NaBr and NaI. Results for the ideal shell model for NaI, assuming only the polarizability of I^-, were reported by Dixon and Sangster.[9,13] Here, we experiment their model which allows for polarization of both ions and also their parametrization[13] for which only I^- is polarizable. We adopt the notation ShM when distinction is not needed, ShM1 for the model which allows only I^- to be polarizable, and ShM2 for the parametrization where both species are polarizable.

The Verlet leapfrog algorithm was used to solve Newton's equations of motion with a time step of 5 fs for the case of the BMHTF RI potential and 2 fs for the case of the adiabatic ShM simulations. For the adiabatic ShM2 of NaI, 10% of the sodium mass was assigned to the shell of Na^+ and 2% of the iodide mass was assigned to the shell of I^-. The same mass was assigned to the shell of I^- for ShM1 while Na^+ was treated as a rigid ion. For NaCl, 10% of the atomic mass was assigned to the shells of both species. This choice was based on the quality of the conservation of energy and the frequencies of the core-shell spring.[17] The systems were equilibrated for 25 ps for the case of the BMHTF potential and 30 ps for the adiabatic ShM simulations. During this period the velocities were scaled for the desired temperatures. The temperatures were chosen to be close to the final temperatures of the HFMD simulations and the densities were those used in the HFMD. The Ewald sum was used for the calculation of the Coulombic interactions. The production stage was run for 25 ps for both simulations. The adiabatic ShM simulations were performed with the code of Fincham, SHELL-DYNAMO,[29] available through the CCP5 program library. Further details on the adiabatic shell model can be found in the article of Mitchell and Fincham.[17]

III. RESULTS AND COMPARISONS

A. Radial distribution functions

The HFMD partial radial distribution functions of NaCl at $T=1058$ K obtained in this work and those at $T=1528$ K previously studied[16] are reported in Fig. 1. A broadening and inward shifting along with the shift of the cutoff position to smaller distances is observed for all partial functions at 1528 K relative to those at the lower temperature. Further, the first maximum of $g_{-+}(r)$ is slightly shifted toward a smaller interionic distance, whereas the first peak of $g_{--}(r)$ is shifted toward a larger distance. These results are in qualitative agreement with the results (not displayed here) obtained from MD of RI and ShM interionic potentials.

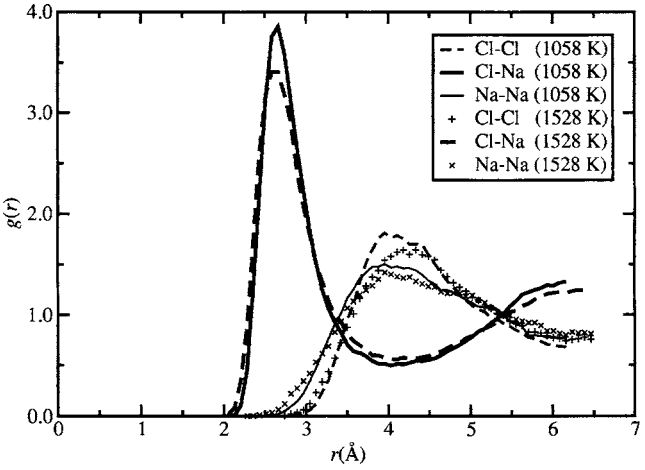

FIG. 1. Partial radial distribution functions of NaCl predicted by HFMD at 1058 and 1528 K.

The partial radial distribution functions of molten NaI predicted by the BMHTF RI, the adiabatic ShM, and HFMD are reported in Fig. 2. The position of cutoff and the position and height of the first maximum of the partial radial distribution functions for NaI are given in Table I. The authors are not aware of any experimental study of the structure of molten NaI and therefore analysis of the HFMD results is restricted to the comparison with the RI and the ShM results.

In Fig. 2 and Table I it can be seen that the main difference between the partial radial distribution functions obtained with ShM1 and ShM2 concerns the heights of $g_{--}(r)$ and $g_{-+}(r)$. In addition, ShM1 predicts a broader function for the I^- like pair function, $g_{--}(r)$.

A comparison of all three partial radial distribution functions obtained through the different MD simulations is given in Fig. 3. The ShM2 results are not included to make comparisons clearer. For $g_{--}(r)$ all RI, ShM1, and the HFMD results are very similar. This was also observed for molten NaCl with the exception of the ShM, which gives results similar to those of the ShM2 for NaI, that is, a sharper and higher peak is predicted.[16] This result is interesting since it suggests that the inclusion of polarizability effects and charge transfer as in HFMD does not affect significantly the like ion pair correlation function of the larger polarizability species relative to a RI potential. The polarizabilities of Cl^- and I^- in the NaCl and NaI crystals (taking the value of the polarizability of Na^+ in the crystal to be the value of Pauling, 0.182 $Å^3$, for the gaseous ion) used by Mayer[4] in deriving the van der Waals coefficients of the BMHTF RI potential and the ShM of Sangtser and Dixon[9] are, respectively, 3.09 and 6.24 $Å^3$ (a value of 3.14 is also reported by Mayer for Cl^- from the empirical scheme used to estimate the polarizability of all halide ions). Those later proposed by Tessmann *et al.*[30] for the electronic polarizabilities of Na^+, Cl^-, and I^- in crystal are, respectively, 0.255, 2.974, and 6.199 $Å^3$. In our previous work[16] we incorrectly referred to the polarizability of Cl^- proposed by Mayer[4] as the free ion polarizability.

This article is copyrighted as indicated in the article. Reuse of AIP content is subject to the terms at: http://scitation.aip.org/termsconditions. Downloaded to IP: 194.117.6.7 On: Sat, 21 Dec 2013 23:21:23

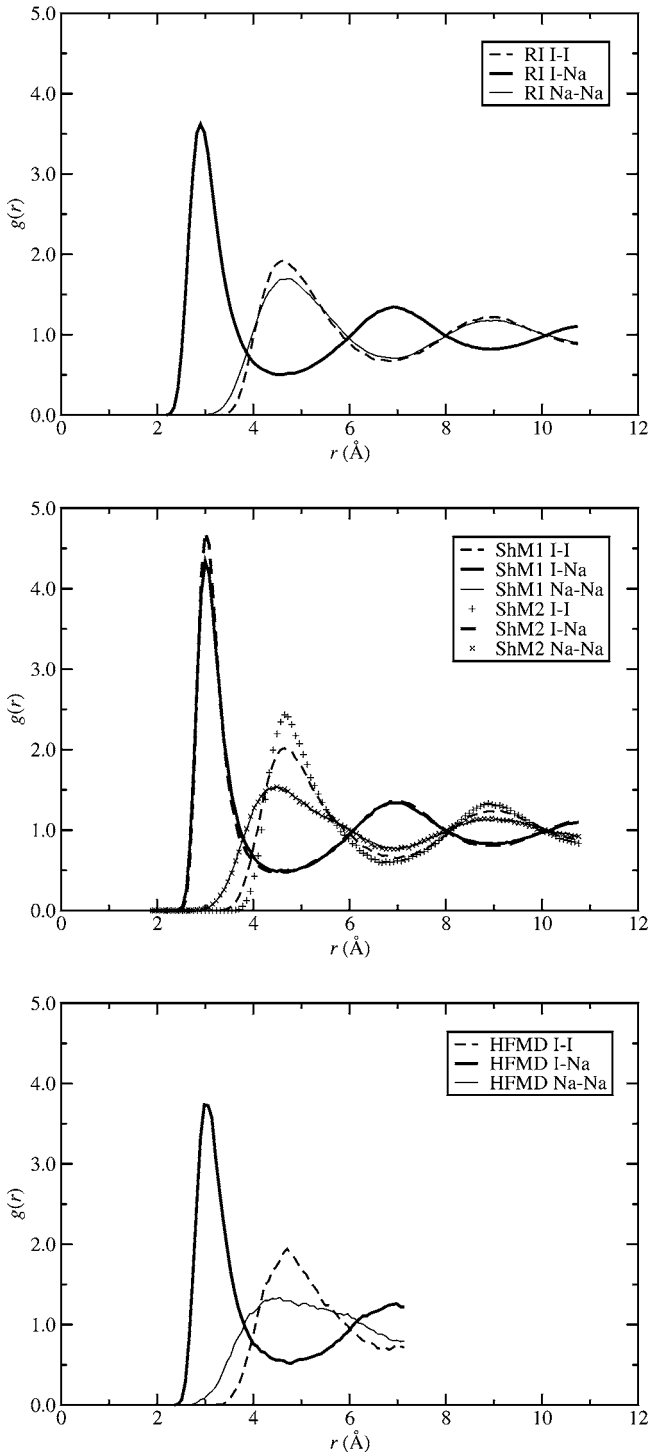

FIG. 2. Partial radial distribution functions of NaI predicted by the BMHTF rigid-ion (RI) model, the adiabatic shell models (ShMs), and HFMD.

Regarding $g_{-+}(r)$ and $g_{++}(r)$ the situation is different. The BMHTF RI interionic potential predicts significantly different results from those of HFMD both for the position and height of the peaks. The ShM1 in turn gives a good agreement with the HFMD results regarding the position of the maxima, although it predicts slightly higher peaks than HFMD. The ShM2 predicts similar positions but significantly higher maxima (see Table I).

Finally, and in agreement with our previous results for NaCl, a larger separation between the like ion correlation functions is predicted by HFMD and ShM, compared with the results from the RI model, for which this separation is essentially related to the anion-cation ionic radius difference. The Tosi-Fumi ionic radii of I^-, Cl^-, and Na^+ considered in the BMHTF RI interionic potential are, respectively, 1.907, 1.585, and 1.170 Å and Pauling's empirical ionic radii for the same ions are 2.16, 1.81, and 0.95 Å.[9]

TABLE I. Comparison of the functions $g_{--}(r)$, $g_{-+}(r)$, and $g_{++}(r)$ for NaI predicted by the BMHTF rigid-ion (RI) model, the adiabatic shell models (ShM1 and ShM2), and HFMD.

MD	T (K)	$g(r)$	Cutoff position (Å)	First maximum position (Å)	First maximum height
RI	1001	g_{--}	3.1	4.6	1.9
		g_{-+}	2.2	2.9	3.6
		g_{++}	2.8	4.8	1.7
ShM1	990	g_{--}	3.3	4.7	2.0
		g_{-+}	2.4	3.0	4.3
		g_{++}	2.8	4.5	1.5
ShM2	996	g_{--}	3.6	4.7	2.4
		g_{-+}	2.5	3.0	4.7
		g_{++}	2.7	4.5	1.5
HFMD	995	g_{--}	3.2	4.7	1.9
		g_{-+}	2.4	3.0	3.7
		g_{++}	2.7	4.5	1.3

Thus, for molten NaI, both ShM and HFMD predict quite similar structures when we compare the position of the first maxima. However, the ShM2 predicts significantly higher peaks, reflecting a more structured liquid. Relative to this latter point the ShM1 is significantly closer to the HFMD results than the ShM2, and this result supports therefore the criticism of Sangster and Dixon regarding their shell model for NaI when the polarizations of both ionic species are included.

B. Self-diffusion coefficients

Figure 4 displays the normalized velocity autocorrelation functions of I^- and Na^+ predicted by the different simulations. Again ShM2 results are omitted for a clearer comparison. A similarity between the ShM1 and HFMD correlations is readily observable. The minimum values from HFMD (Na^+: −0.17 and I^-: −0.17) are significantly closer to those of the ShM1 (Na^+: −0.20 and I^-: −0.19) than the RI (Na^+: −0.28 and I^-: −0.098) minima. For ShM2 (Na^+: −0.22 and I^-: −0.21) the minima are slightly deeper than for ShM1. HFMD predicts the largest times for both I^- and Na^+ to reach the minimum (Na^+: 0.13 ps and I^-: 0.36 ps) corresponding to the maximum anticorrelation. The situation is similar for the case of molten NaCl at 1058 and 1528 K.

The self-diffusion coefficients obtained through Green-Kubo integration for NaI and NaCl are compared to available experimental data in Tables II and III, respectively. The self-diffusion coefficient of Na^+ in NaI is overpredicted by HFMD, whereas that of I^- is in good agreement with experimental data. For NaCl (see Table III) the coefficients of both species are overpredicted by HFMD relatively to low tem-

This article is copyrighted as indicated in the article. Reuse of AIP content is subject to the terms at: http://scitation.aip.org/termsconditions. Downloaded to IP: 194.117.6.7 On: Sat, 21 Dec 2013 23:21:23

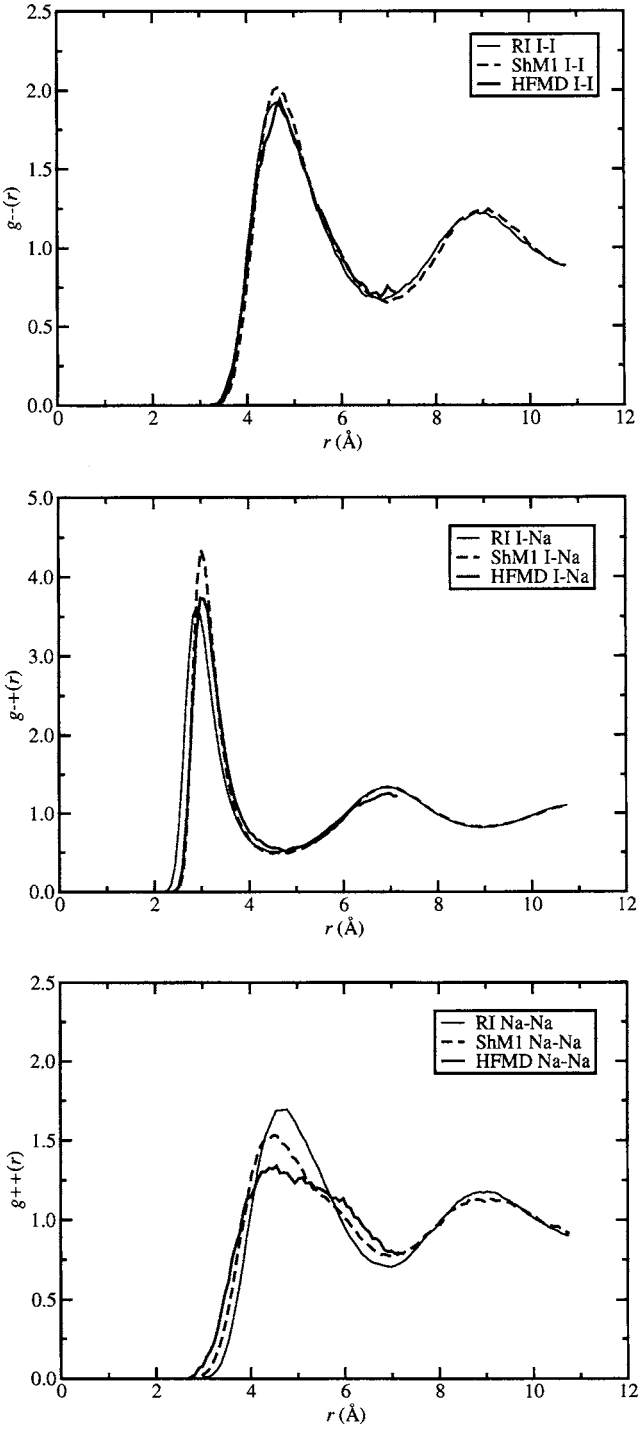

FIG. 3. Comparison of the functions $g_{--}(r)$, $g_{-+}(r)$, and $g_{++}(r)$ for NaI predicted by the BMHTF rigid-ion (RI) model, the adiabatic shell model (ShM1), and HFMD.

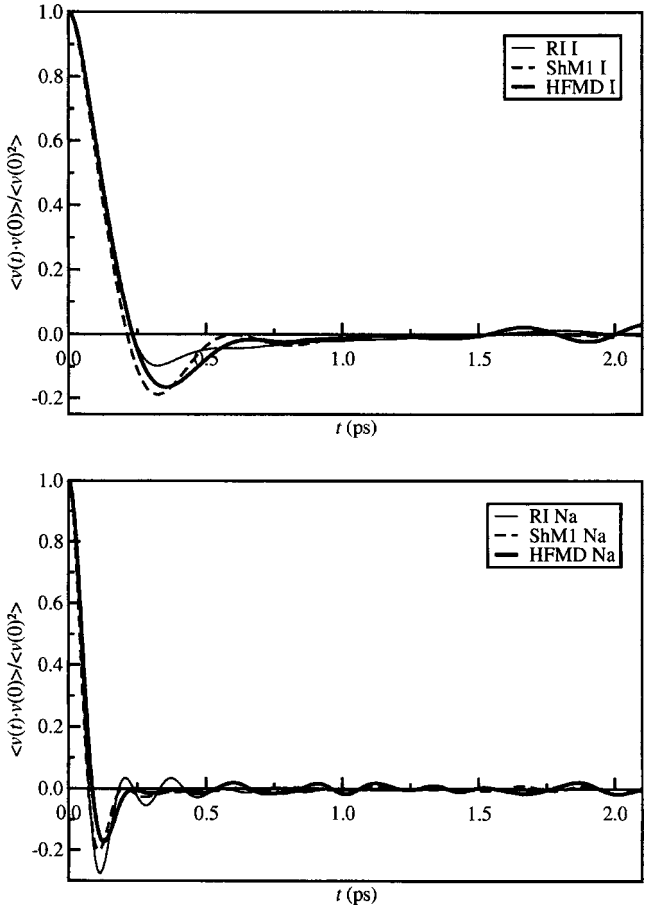

FIG. 4. Normalized velocity autocorrelation function of I^- and Na^+ predicted by the BMHTF rigid-ion (RI) model, the adiabatic shell model (ShM1), and HFMD.

perature extrapolations of experimental data. The ShM2 underestimates the self-diffusion coefficients of I^- and Na^+ in NaI, and the ShM for NaCl (which allows for polarization of both species) also underestimates the self-diffusion of the two ionic species. However, the ShM1 prediction of the self-diffusion coefficient of Na^+ is in good agreement with experimental data, while that of I^- is slightly underpredicted. Regarding the BMHTF RI interionic potential, the self-diffusion coefficients for I^- and Cl^- are in good agreement with experimental data, whereas self-diffusion of Na^+ is underpredicted for both salts. The RI potential predicts a smaller difference between the self-diffusion coefficients of the anions and cations when compared to both HFMD and ShM. It should be observed that the HFMD results for the self-diffusion coefficients are based on the calculation of the velocity autocorrelation functions averaged over 32 particles and 1700 time steps, and consequently, they are less accurate than those from the classical simulations. Moreover, experimental data for the cations appear to have a larger uncertainty, especially for NaCl, given the differences between different experimental studies. However, the lower experimental values for NaCl (Ref. 31) (Table III) are considered the most accurate by the authors of those experiments.[31–33]

C. Electronic density analysis: Hirshfeld charge partitioning

With the purpose of analyzing charge fluctuations in ionic systems such as alkali halides, Hirshfeld[18] atomic charges were estimated from the electronic density of selected HFMD configurations for NaI and NaCl. This analysis is based on 58 configurations (0.125 ps spaced) for NaI (T=995 K) and NaCl (T=1058 and 1528 K).

The Hirshfeld[18] electron density partitioning method decomposes the molecular electron density $\rho_M(\mathbf{r})$ into atomic contributions $\rho_A(\mathbf{r})$, which are proportional to the weight $w_A(\mathbf{r})$ of the electron density of the isolated atoms $\rho_A^0(\mathbf{r})$ in a

This article is copyrighted as indicated in the article. Reuse of AIP content is subject to the terms at: http://scitation.aip.org/termsconditions. Downloaded to IP: 194.117.6.7 On: Sat, 21 Dec 2013 23:21:23

TABLE II. Green-Kubo self-diffusion coefficients of I^- and Na^+ from RI, ShM, and HFMD simulations.

	T (K)	D_{Na^+} (10^{-3} cm^2 s^{-1})	$D^{Expt.}_{Na^+}$ (10^{-3} cm^2 s^{-1})	D_{I^-} (10^{-3} cm^2 s^{-1})	$D^{Expt.}_{I^-}$ (10^{-3} cm^2 s^{-1})
RI	1001	0.075	0.087[a]	0.050	0.050[a]
			0.083[b]		0.047[b]
ShM1	990	0.081	0.085[a]	0.040	0.048[a]
			0.081[b]		0.046[b]
ShM2	996	0.064	0.086[a]	0.026	0.049[a]
			0.082[b]		0.046[b]
HFMD	995	0.12	0.086[a]	0.048	0.049[a]
			0.082[b]		0.046[b]

[a]Experimental data are from Ref. 40.
[b]Experimental data are from Ref. 32.

promolecule electron density, $\rho_M^{Pro}(\mathbf{r})$. This fictitious promolecule electron density, in turn, is obtained from superposition of the electron density of the isolated atoms at the positions the atoms occupy in the real molecule, $\rho_M^{Pro}(\mathbf{r})=\Sigma_A\rho_A^0(\mathbf{r})$. The weight factor is defined by the ratio, $w_A(\mathbf{r})=\rho_A^0(\mathbf{r})/\rho_M^{Pro}(\mathbf{r})$, and the Hirshfeld charges Q_A^H are obtained from

$$Q_A^H = Z_A - \int dr^3 w_A(\mathbf{r})\rho_M(\mathbf{r}), \tag{1}$$

where Z_A is the atomic number (nuclear charge). Within a pseudopotential description Z_A is replaced by the charge of the pseudoions, $Z_{ion}=Z_A-(Z_A-N_e^{PP})$, where N_e^{PP} is the number of electrons considered in the construction of the pseudopotentials, which for the TM pseudopotentials are the valence electrons. However, all-electron atomic densities $\rho_A^0(\mathbf{r})$ are used to calculate the promolecule electron density $\rho_M^{Pro}(\mathbf{r})$ and the weight factors $w_A(\mathbf{r})$ of Eq. (1). The Hirshfeld method was demonstrated to correspond to a situation where atoms in molecules conserve a maximal information relative to the isolated atoms.[34] This means that the Hirshfeld partitioning method divides the molecular electron density into atomic contributions in such a way that the lost of the isolated atom identity (as defined by their electron density) in a molecule is minimized.

Equation (1) for atoms in molecules can also be applied to the analysis of the electron density of bulk crystals[35,36] or liquids. For NaCl, the Hirshfeld charges in solid phase and in the isolated NaCl molecule were calculated at the PBE/TM theoretical level. The lattice constant value considered was 5.66 Å.[16] The equilibrium distance of gas phase NaCl was presently estimated as 2.36 Å by using a cubic supercell, 28.8 Å side length, which is large enough to avoid significant interaction with image particles. The calculated binding energy for NaCl is −4.18 eV which underestimates the experimental value of −5.57 eV.[37] The experimental lattice constant (at 0 K) and equilibrium distance for the NaCl molecule are, respectively, 5.60 (Ref. 38) and 2.36 Å.[37] The magnitude of the Hirshfeld charge, $|Q_-^H|=|Q_+^H|$, in the solid is $0.146e$ and for the NaCl molecule is $0.520e$.

Hirshfeld charges for solid CaF_2 were reported by Verstraete and Gonze.[35] The authors found the Hirshfeld charges to be sensitive to the functional/pseudopotential combination, although the order of magnitude and the direction of charge transfer are consistent (see Ref. 35 for details).

Here, our main interest is to analyze the distribution of

TABLE III. Green-Kubo self-diffusion coefficients of Cl^- and Na^+ from RI, ShM, and HFMD simulations. The experimental values given in Ref. 31 are considered the most accurate by the authors of the experiments (Refs. 31–33).

	T (K)	D_{Na^+} (10^{-3} cm^2 s^{-1})	$D^{Expt.}_{Na^+}$ (10^{-3} cm^2 s^{-1})	D_{Cl^-} (10^{-3} cm^2 s^{-1})	$D^{Expt.}_{Cl^-}$ (10^{-3} cm^2 s^{-1})
RI	1067	0.067	0.072[a]	0.060	0.057[a]
			0.083[b]		0.058[b]
			0.12[c]		0.060[c]
ShM	1072	0.063	0.074[a]	0.043	0.058[a]
			0.084[b]		0.059[b]
			0.12[c]		0.061[c]
HFMD	1058	0.10	0.070[a]	0.078	0.056[a]
			0.080[b]		0.056[b]
			0.12[c]		0.058[c]

[a]Low temperature extrapolations from the experimental equation given in Ref. 31.
[b]Low temperature extrapolations from the experimental equation given in Ref. 32.
[c]Low temperature extrapolations from the experimental equation given in Ref. 33.

This article is copyrighted as indicated in the article. Reuse of AIP content is subject to the terms at: http://scitation.aip.org/termsconditions. Downloaded to IP: 194.117.6.7 On: Sat, 21 Dec 2013 23:21:23

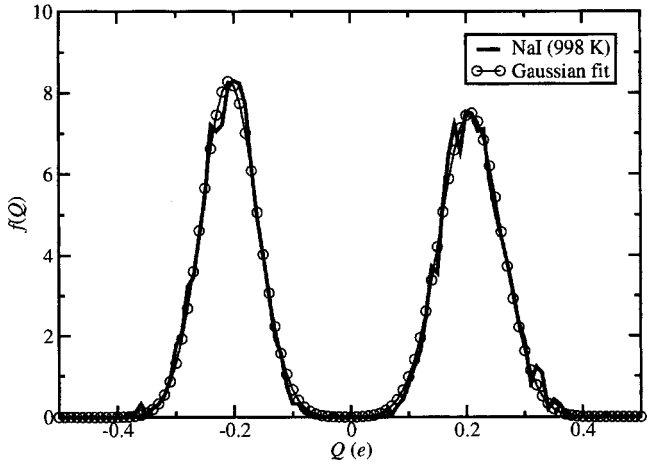

FIG. 5. Hirshfeld charge distribution for NaI from HFMD (995 K) and corresponding fitted Gaussian function.

ionic charges in liquid phase related to the time dependent fluctuations of the electronic density. Therefore, emphasis will be placed on the shape and thermodynamic state dependence of the Hirshfeld charge distribution rather than the average values of the charges.

Figure 5 displays the Hirshfeld charge distribution calculated for NaI, and Fig. 6 gives the charge distributions for molten NaCl at two distinct temperatures. The function $f(Q)$

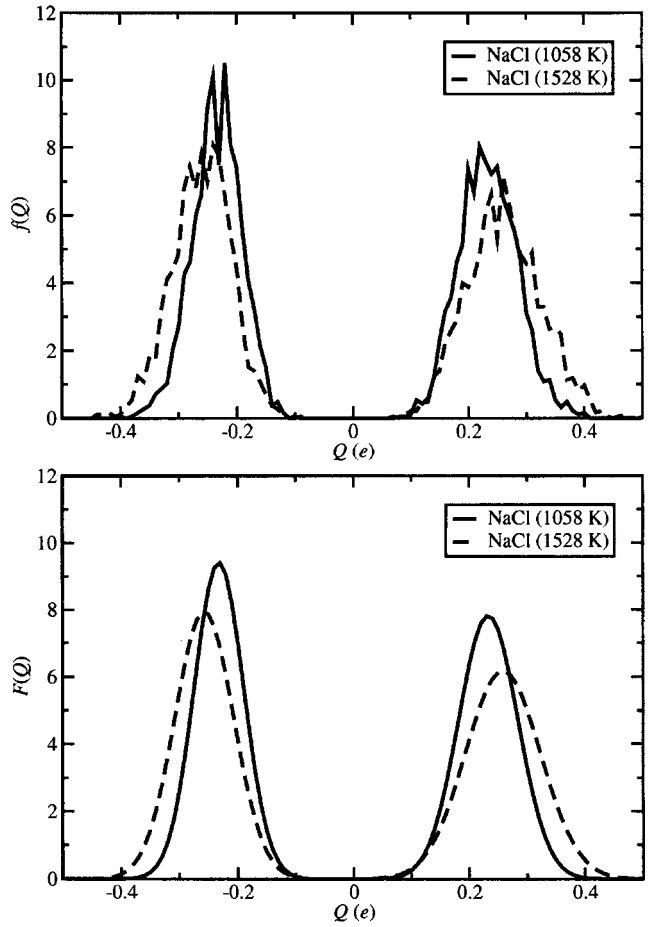

FIG. 6. Hirshfeld charge distributions for NaCl from HFMD at two temperatures (1058 and 1528 K) and corresponding fitted Gaussian functions.

TABLE IV. Gaussian function fitted parameters for the NaI and NaCl Hirshfeld charge distributions of Figs. 5 and 6.

Molten salt	T (K)	Species	$\langle Q^H \rangle (e)$	$\sigma(e)$
NaI	995	I	−0.21	0.048
		Na	+0.21	0.053
NaCl	1058	Cl	−0.23	0.042
		Na	+0.23	0.051
NaCl	1528	Cl	−0.26	0.050
		Na	+0.26	0.065

in Figs. 5 and 6 is given by $f(Q)=\langle N(Q\pm dQ)\rangle/NdQ$, where $N(Q\pm dQ)$ is the number of ions, for a given configuration, with charge falling inside $(Q\pm dQ)$, N is the number of ions, and dQ is the infinitesimal charge interval considered for counting $N(Q\pm dQ)$. The $\langle\ \rangle$ denotes the average over the number of configurations. Figures 5 and 6 also report fitted Gaussian distribution functions to the Hirshfeld charge distributions. Table IV gives the fitted values of the average charge $\langle Q^H \rangle$ and the width (standard deviation) σ of the Gaussian distribution functions. The predicted average charges for NaI and NaCl are very low, in keeping with the fact that Hirshfeld charges are, in general, significantly lower than those obtained through other partitioning methods.[35,36,39] Low Hirshfeld charges are also obtained when all-electron atom descriptions are considered.[39] From Figs. 5 and 6 and Table IV several conclusions can be drawn: (1) the magnitudes of Hirshfeld charge transfer in molten NaI and NaCl are similar, although a slightly larger average charge is observed for NaCl, (2) the charge transfer slightly increases with the temperature (and the decrease of the density) for molten NaCl, (3) the increase of the charge transfer with temperature is coupled to an increase of the width of the charge distribution, and (4) the width of the charge distribution functions is larger for the cation for both molten NaCl and NaI. This last point is perhaps the most difficult to interpret since, intuitively, a larger width could be expected for the more polarizable species. The fluctuations of charge are related to the distortion of the electron cloud around the nuclei. Hence, since both Cl^- and I^- have significantly larger dipole polarizabilities than Na^+ and Hirshfeld charges result from a direct analysis of the electron density, we are led toward the idea that larger charge fluctuations must take place for the more polarizable species. The results of Hirshfeld charge analysis, however, predict the charges of the anions to be less disperse than those of the cations. It is difficult to say whether this result is related to the Hirshfeld partitioning method, to the pseudoatom description, or our intuition, based on the gas phase polarizability, is not adequate for condensed phase, where many-body and confinement effects play a significant role.

Finally, assuming that the predicted width of the Hirshfeld charge distributions is correct in the sense that it reflects the charge transfer fluctuations in molten NaI and NaCl, we want to know what is the effect of these charge distributions on the structure and dynamics of the molten salts. To study this effect we have carried MD simulations of the BMHTF

This article is copyrighted as indicated in the article. Reuse of AIP content is subject to the terms at: http://scitation.aip.org/termsconditions. Downloaded to IP: 194.117.6.7 On: Sat, 21 Dec 2013 23:21:23

RI interionic potential using polydisperse charges for the anion and cation assigned from the Gaussian charge distribution functions displayed in Figs. 5 and 6. We have centered the charge distributions around +1 and −1, however, which are the values used in both RI and ShM MD simulations. The radial distribution functions and self-diffusion coefficients calculated this way do not show any significant differences relative to RI simulations with equal charges for all ions. The reasons are the small width of the Hirshfeld charge distributions and the fact that the charge distribution widths for the anionic and cationic species are very similar. Hence, and assuming that this is a reasonable approach to isolate charge transfer effects on a MD simulation, we can conclude that differences between RI and experimental results, for both structure and self-diffusion coefficients, are mainly related to polarization effects.

IV. CONCLUSIONS

First principles Hellmann-Feynman molecular dynamics of molten NaI and NaCl are reported. The PBE GGA functional is used for the XC functional, and norm-conserving pseudopotentials of the Troullier-Martins type are applied to describe the interaction between the valence electrons and the nuclei and core electrons. The radial distribution functions and self-diffusion coefficients are compared to those predicted by the BMHTF rigid-ion and shell-model potentials. A shell-model interionic potential which allows for polarization of I^- predicts a similar structure to that of HFMD for NaI regarding the position of the peaks, although a more structured melt is predicted. The inclusion of polarization on the Na^+ ion leads to an even more structured description of molten NaI, also manifested through a decrease of the self-diffusion coefficients of the two ionic species. The self-diffusion coefficients estimated by HFMD are significantly larger than experimental values except for the I^- ion. HFMD results for NaCl at $T=1058$ K overestimate experimental results for the self-diffusion coefficients, whereas those at a higher temperature ($T=1528$ K) previously reported[16] are below those of the experiment, especially for the anionic species. Hirshfeld charge distributions are computed from HFMD configurations for molten NaI and NaCl. The charge distributions for NaCl at two temperatures indicate a small increase of the charge transfer with temperature, as well as the broadening of the charge distribution. The combined results from HFMD and Hirshfeld charges support the views that the differences observed between the like ion pair correlation functions in molten NaI and NaCl can be mainly related to polarization effects and that charge transfer only plays a minor role.

ACKNOWLEDGMENTS

The authors would like to acknowledge Dr. Matthieu Verstraete at the University of York for his help on the calculation of the atomic electronic densities with the program FHI98. One of the authors (N.G.) would also like to acknowledge a fellowship support from Fundação para a Ciência e Tecnologia (FCT) from Portugal for a postdoctoral grant (No. SERH/BPD/14875/2003). This work was partially supported by FCT (No. POCI/MAT/55977/2004).

[1] F. G. Edwards, J. E. Enderby, R. A. Howe, and D. I. Page, J. Phys. C **8**, 3483 (1975).
[2] F. Lantelme, P. Turq, B. Quentrec, and J. W. E. Lewis, Mol. Phys. **28**, 1537 (1974).
[3] M. V. Born and J. E. Mayer, Zeits. f. Physik **75**, 1 (1932).
[4] J. E. Mayer, J. Chem. Phys. **1**, 270 (1933).
[5] M. L. Huggins and J. E. Mayer, J. Chem. Phys. **1**, 643 (1933).
[6] M. P. Tosi and F. G. Fumi, J. Phys. Chem. Solids **25**, 45 (1964).
[7] F. G. Fumi and M. P. Tosi, J. Phys. Chem. Solids **25**, 31 (1964).
[8] M. Dixon and M. J. L. Sangster, J. Phys. C **9**, L5 (1976).
[9] J. L. Sangster and M. Dixon, Adv. Phys. **25**, 247 (1976).
[10] S. Biggin and J. E. Enderby, J. Phys. C **15**, L305 (1982).
[11] L. V. Woodcock, in *Advances in Molten Salt Chemistry*, edited by J. Braunstein, G. Mamantov, and G. P. Smith (Plenum, New York, 1975), Vol. 3, p. 1.
[12] L. V. Woodcock and K. Singer, Trans. Faraday Soc. **67**, 12 (1971).
[13] M. Dixon and M. J. L. Sangster, J. Phys. C **8**, L8 (1975).
[14] G. Jacucci, I. R. McDonald, and A. Rahman, Phys. Rev. A **13**, 1581 (1976).
[15] M. Wilson and P. A. Madden, J. Phys.: Condens. Matter **5**, 2687 (1993).
[16] N. Galamba and B. J. Costa Cabra, J. Chem. Phys. **126**, 124502 (2007).
[17] P. J. Mitchell and D. Fincham, J. Phys.: Condens. Matter **5**, 1031 (1993).
[18] F. L. Hirshfeld, Theor. Chim. Acta **44**, 129 (1977).
[19] W. Kohn and L. J. Sham, Phys. Rev. **140**(4A), A1133 (1965).
[20] P. Hohenberg and W. Kohn, Phys. Rev. **136**(3B), B864 (1964).
[21] S. Goedecker, SIAM J. Sci. Comput. (USA) **18**, 1605 (1997).
[22] M. C. Payne, M. P. Teter, D. C. Allan, T. A. Arias, and J. D. Joannopoulos, Rev. Mod. Phys. **64**, 1045 (1992).
[23] X. Gonze, Phys. Rev. B **54**, 4383 (1996).
[24] J. Perdew, K. Burke, and M. Ernzerhof, Phys. Rev. Lett. **77**, 3865 (1996).
[25] N. Troullier and J. L. Martins, Phys. Rev. B **43**, 1993 (1991).
[26] S. G. Louie, S. Froyen, and M. L. Cohen, Phys. Rev. B **26**, 1738 (1982).
[27] M. Fuchs and M. Scheffler, Comput. Phys. Commun. **119**, 67 (1999).
[28] G. J. Janz, NIST Properties of Molten Salts Database (NIST SRD 27, Boulder, CO, 1992).
[29] D. Fincham, J. Mol. Graphics **12**, 29 (1994).
[30] J. R. Tessman, A. H. Kahn, and W. Shockley, Phys. Rev. **92**, 890 (1953).
[31] J. O. M. Bockris, S. R. Richards, and L. Nanis, J. Phys. Chem. Solids **69**, 1627 (1965).
[32] J. O. M. Bockris and G. W. Hooper, Discuss. Faraday Soc. **32**, 218 (1961).
[33] A. Z. Borucka, J. O. M. Bockris, and J. A. Kitchener, Proc. R. Soc. London, Ser. A **241**, 554 (1957).
[34] R. F. Nalewajski and R. G. Parr, Proc. Natl. Acad. Sci. U.S.A. **97**, 8879 (2000).
[35] M. Verstraete and X. Gonze, Phys. Rev. B **68**, 195123 (2003).
[36] J. Meister and W. H. E. Schwarz, J. Phys. Chem. **98**, 8245 (1994).
[37] T. P. Martin, Phys. Rep. **95**, 167 (1983).
[38] H. J. F. Jansen and A. J. Freeman, Phys. Rev. B **33**, 8629 (1986).
[39] F. De Proff, C. Van Alsenov, A. Peeters, W. Langenaeker, and P. Geerlings, J. Comput. Chem. **23**, 1198 (2002).
[40] S. B. Tricklebank, L. Nanis, and J. O. M. Bockris, J. Phys. Chem. **68**, 58 (1964).

This article is copyrighted as indicated in the article. Reuse of AIP content is subject to the terms at: http://scitation.aip.org/termsconditions. Downloaded to IP: 194.117.6.7 On: Sat, 21 Dec 2013 23:21:23